

## RESEARCH ARTICLE



# Over-the-Air Modulation Classification using Deep Learning in Fading Channels for Cognitive Radio

**OPEN ACCESS****Received:** 02.12.2021**Accepted:** 23.12.2021**Published:** 24.12.2021K R Arjun<sup>1\*</sup>, T P Surekha<sup>2</sup><sup>1</sup> Research Scholar, Department of Electronics & Communication, Vidyavardhaka College of Engineering, Mysore, 570002, India<sup>2</sup> Professor, Department of Electronics & Communication, Vidyavardhaka College of Engineering, Mysore, 570002, India

**Citation:** Arjun KR, Surekha TP (2021) Over-the-Air Modulation Classification using Deep Learning in Fading Channels for Cognitive Radio. Indian Journal of Science and Technology 14(46): 3360-3369. <https://doi.org/10.17485/IJST/v14i46.2073>

\* **Corresponding author.**

[arjunkrmys@gmail.com](mailto:arjunkrmys@gmail.com)

**Funding:** None

**Competing Interests:** None

**Copyright:** © 2021 Arjun & Surekha. This is an open access article distributed under the terms of the [Creative Commons Attribution License](https://creativecommons.org/licenses/by/4.0/), which permits unrestricted use, distribution, and reproduction in any medium, provided the original author and source are credited.

Published By Indian Society for Education and Environment ([iSee](https://www.indjst.org/))

**ISSN**

Print: 0974-6846

Electronic: 0974-5645

## Abstract

**Background/Objectives:** The ability to recognize the type of modulation is a critical function of Cognitive Radio. The objective of this study is to increase the modulation classification efficiency in Over-The-Air (OTA) signals by utilizing channel characteristics that are strong. **Methods:** In this work, we demonstrate how to classify Over-The-Air modulation using a deep learning technique under various fading channels simulating real-time data. The network recognizes eight different digital modulation schemes and three different analogue modulation methods. Each modulation scheme will consist of 10,000 frames with 1024 samples per frame and a sampling rate of 200 kHz. Each sample will pass through fading channels prior to training, with 80% of samples are for training, 10% for validation, and 10% for testing. Six convolutional layers and one fully linked layer comprise our network. The final convolution layer is followed by a batch normalization layer, an activation layer utilizing rectified linear units (ReLU), and a maximum pooling layer. As a result, the final convolution layer contains soft-max activation instead of the maximum pooling layer. **Findings:** Modulation categorization OTA is done with two separate ADALM-PLUTO SDRs working in various channel configurations. Network-I has a forecast accuracy of 91.4 percent using 12 Mini-Batch Size and 256 Epochs, whereas Network-II has a prediction accuracy of 95.3 percent using 24 Mini-Batch Size and 128 Epochs. There are a number of ways in which SDR technology can aid to make computer-generated data more realistic, such as adopting alternative channel models. **Novelty:** Using Software Defined Radio hardware; the same network was used to analyze various fading situations, such as Rayleigh, Rician or Lognormal distributions, and to optimize the network topology by adjusting hyper-parameters to increase accuracy.

**Keywords:** Cognitive Radios (CR); Fading Channel; OTA; SDR; and Modulation

## 1 Introduction

As a result of the exponential rise of portable devices over the past two decades, there has been an unavoidable problem of spectrum scarcity<sup>(1)</sup>. It is also clear from several Federal Communications Commission (FCC) studies that the vast majority of the spectrum that has been allotted is being underutilized. Cognitive Radio (CR) is one of the solutions to overcome the problem of spectrum underutilization. In its most basic form and as a part of primary objective, CR must be able to identify unutilized spectrum that was initially assigned to a Primary User (PU) or Licensed User (LU) and reallocate it to a Secondary User (SU) or Unlicensed User (UU) who requests service<sup>(2)</sup>. The second objective is to manage a network using information learned from the first. Additionally, Spectrum Allocation and radio parameter tuning are part of the second phase of the task as shown in Figure 1.

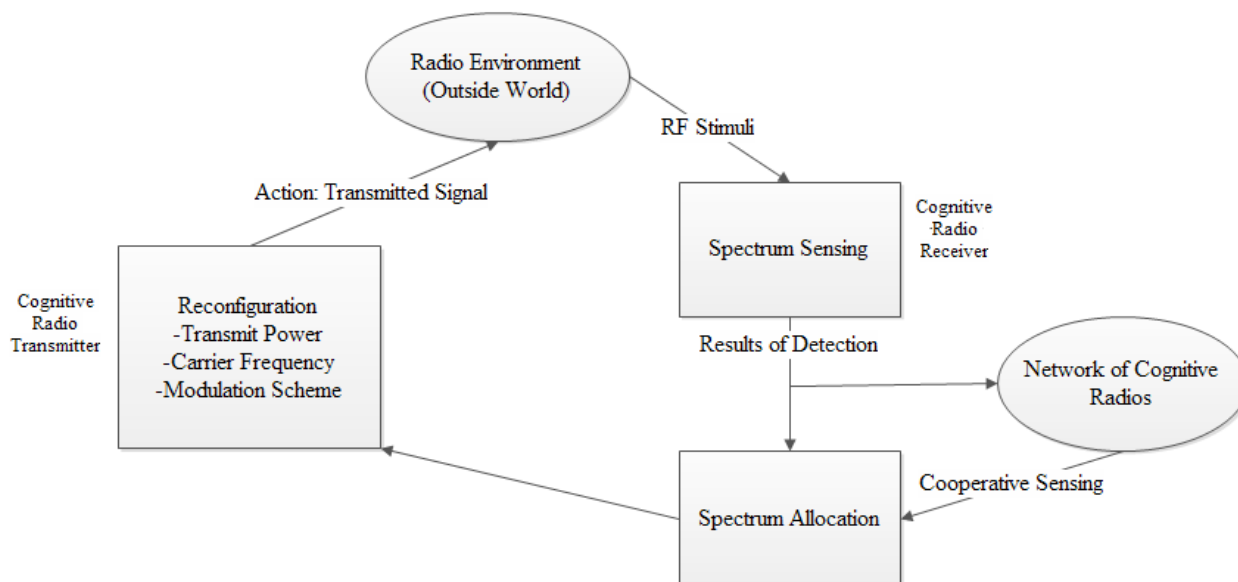


Fig 1. Cognitive Radio Cycle

Modulation of signals is a critical step in wireless communication systems. The majority of the times both signal identification and demodulation, modulation recognition tasks are used<sup>(3)</sup>. In recent years, however, the number of modulation methods and parameters used in wireless communication systems has increased dramatically. Thus, the difficulty of precisely recognizing modulation schemes becomes more difficult. The challenge of CR is to identify and differentiate<sup>(4)</sup> various radio signals which has different demands and behaviors under fading channels that may occur due to user mobility. CR systems face the challenge of detecting a radio signal’s modulation type in order to determine what type of communication scheme and transmitter is there. Convolutional neural networks (CNNs) have recently been used to the job of radio modulation identification in order to introduce the notion of deep learning<sup>(5-8)</sup>.

There has been a lot of recent pioneering work on the use of deep learning to extract signal characteristics and demonstrate the feasibility of utilizing convolutional neural networks (CNNs) for modulation classification. Various techniques like implementing ANN with multiple detectors’ test statistics (TSs)<sup>(9)</sup>, Comparison of DL-based estimator with BEM-LMMSE estimator<sup>(10)</sup>, Doubly Selective Fading Channel Estimation Using Deep Learning<sup>(11)</sup>, and combining various CNNs to increase the Modulation Classification accuracy<sup>(12)</sup> has been proposed. Over-The-Air (OTA) signals with Software Defined Radio (SDR) hardware has been demonstrated where the duration of observation<sup>(13,14)</sup> is short time. In<sup>(15)</sup>, Authors regarded spectrum sensing as a two-category classification problem and offered a deep learning approach. The results of the simulation reveal that the proposed technique is more successful than the conventional approach. It is also capable of adapting to a wide range of untrained signals, as demonstrated by the approach proposed by authors.

Based on the findings of comparable studies, it is clear that the modulation classification accuracy reached by simulation is higher than the accuracy gained when the same technique is applied to real-time OTA signals. Previous research has shown that, in order to replicate a real-time scenario, the training dataset must be subjected to a variety of channel circumstances, as well as diverse testing settings. In our research, we have discovered these gaps and developed a strategy to improve the modulation

classification accuracy in OTA signals by simulating various channel circumstances in real time.

On the rest of the paper: A quick simulation of wireless channels in data set generation is provided in Section 3. Sections 4 and 5 of this document describe the Deep Learning-based Modulation categorization algorithm and the Over-the-Air testing methodology. Results, discussion, and conclusion appear in sections 6 and 7 of the paper.

## 2 Wireless channel models

The variation in channel strength across time and frequency is a defining feature of the mobile wireless channel. The differences can be classified into two broad categories:

1. Fading on a large scale, caused by signal path loss as a function of distance and the amount of shadow cast by large objects such as buildings and mountains. This transpires when the mobile device travels an equivalent distance to the size of the cell and is frequently independent of frequency.
2. Small-scale fading occurs as a result of the various signal routes between the transmitter and receiver interfering constructively and destructively. This occurs on a spatial scale comparable to the wavelength of the carrier and is dependent on frequency.

It is possible for the received signal power to fluctuate by 30-40 dB when the receiver is moved by a quarter of a wavelength in small-scale fading. An increasing number of paths are available in a mobile-radio environment because of Doppler shifts, delays and path attenuation, which results in a time-varying signal. This is a time-varying linear channel. Rayleigh fading is another name for small-scale fading because, when the number of copies of the bit stream arrive at slightly different times is significant; the envelope of the received signal is quantitatively characterized by a Rayleigh distribution. If a component with direct line of sight exists, it is characterized by a Rician distribution. The fading patterns of a radio signal are described by the statistics distributions in next section.

### 2.1 Rician Distribution

It is Rician when a dominant stationary (nonfading) signal component is present, like a LOS propagation channel. The Rician distribution's probability density function is given by<sup>(16)</sup>:

$$p(r) = \frac{r}{\sigma^2} e^{-\left(\frac{r^2 + A_r^2}{2\sigma^2}\right)} I_0\left(\frac{A_r r}{\sigma^2}\right) \quad \text{for } A \geq 0, r \geq 0 \quad (1)$$

where:  $A_r$  = Dominating signal amplitude and

$I_0$  = Bessel modified First-order function and zero order

$\frac{r^2}{2}$  = instantaneous power

$\sigma$  = local power standard deviation

The Rician distribution is frequently characterized in terms of a parameter K, known as the Rician factor, which is denoted as:

$$K = 10 \log \frac{A^2}{2\sigma^2} \text{ dB} \quad (2)$$

### 2.2 Rayleigh Distribution

The Rayleigh distribution is employed in order to characterize the statistical time-varying nature of the received envelope of a flat fading signal or the envelope of an individual multipath component. The Rayleigh distribution is represented by the symbol<sup>(16)</sup>:

$$p(r) = \frac{r}{\sigma^2} e^{-\left(\frac{r^2}{2\sigma^2}\right)} \quad 0 \leq r \leq \infty \quad (3)$$

where:  $\sigma$  = received signal rms value

$\frac{r^2}{2}$  = instantaneous power

$\sigma^2$  = local power standard deviation

### 2.3 Lognormal Distribution

With identical transmitter and receiver spacing but variable levels of propagation congestion, the lognormal distribution depicts random shadowing effects. Lognormal distribution is represented by:

$$p(r) = \frac{1}{\sqrt{2\pi\sigma_s}} e^{-\left[\frac{(S - S_m)^2}{2\sigma_s^2}\right]} \tag{4}$$

where:  $S_m$  = mean value of  $S$  in dBm  
 $\sigma_s$  = standard deviation of  $S$  in dB  
 $S = 10 \log$  in dBm  
 $s$  = Signal power in mW

### 3 Deep Learning based Modulation Classification

In order to learn usable visualizations of characteristics derived from data, deep learning employs neural networks. The nonlinear processing layers of neural networks are made up of simple parts that operate in parallel and are based on the structure of the human nervous system. When it comes to object classification, deep learning models can sometimes outperform humans.

Recently, the Convolutional Neural Network (CNN) has been found to be an effective tool for image categorization and audio signal processing. This technology has also been successfully applied in other fields, such as video detection and natural language processing. A simple CNN architecture was used to distinguish between 10 distinct modulations as a result of its improved performance in the extraction of features. The simulation findings reveal that CNN not only gives superior accuracy outcomes, but also provides more flexibility than current expert-based approaches<sup>(17)</sup>.

As illustrated in Figure 2<sup>(18)</sup>, Networks that use Deep Neural Networks are made up of a number of hidden layers. These networks are capable of handling not only unstructured and unlabeled input, but also non-linearity. They, like the human brain, have a hierarchical structure of neurons. According to the input received, the neurons transmit the signal to other neurons. If the signal value exceeds the threshold value, the output is passed; otherwise, it is ignored. As you can see, data is transferred to the input layer, which generates output for the following layer, and so on until it reaches the output layer, which delivers a yes or no forecast based on probability. Each layer is composed of several neurons, and each neuron performs a function known as the Activation Function. They serve as a conduit for signal transmission to the next linked neuron. The weight has an effect on the output of the following neuron and, finally, on the final output layer. Although the initial weights are random, as the network is trained iteratively, the weights are optimized to ensure that the network provides an accurate forecast.

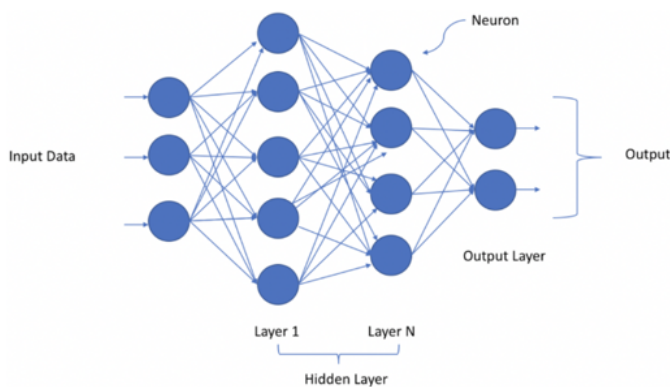


Fig 2. Structure of Deep Neural Network

Representing the received signal as a time series as an input to an N-class decision problem, we can classify the modulation. At each discrete time step via an analogue to digital converter, A radio signal is sampled in-phase and quadrature and generate a 1xN complex valued vector. A time series signal,  $s(t)$ , can be either continuous or sine waves with varying frequencies, phases, amplitudes, or other permutations of several of them modulated onto a sinusoid.  $n(t)$  in equation 5, is a Gaussian white noise process that is added to the signal to account for thermal noise.

$$r(t) = s(t) * c + n(t) \tag{5}$$

Many expert features and decision statistics are developed analytically using this simplified formula, although the real-world relationship often looks more like that given by equation (6).

$$r(t) = e^{j*nL_o(t)} \int_{\tau=0}^{\tau_0} s(n_{clk}(t-\tau))h(\tau) + n_{Add}(t) \quad (6)$$

Several real-world effects that are difficult to model are taken into account: random walk modulation of the residual carrier,  $nL_o(t)$ , random walk using a residual clock oscillator as a sampling method,  $n_{clk}(t)$ , channel impulse response that changes over time and is not constant in amplitude  $h(t-\tau)$ , and Networks for Recognizing Convolutional Radio Modulation 3 other sources of noise that may or may not be white,  $n_{Add}(t)$ . Each has a time-varying source of inaccuracy that is not understood.

## 4 Methodology

In this paper, we classify modulation using a convolutional neural network (CNN). Following that, synthetic, channel-impaired waveforms are generated. We train a CNN for modulation categorization using the produced waveforms as training data. Finally, validate the CNN using SDR hardware and over-the-air signals.

### 4.1 Dataset Generation

Synthetic radio communications signals are created in the same deterministic way as real systems, including modulation, pulse shaping, sent data, and other well-defined send characteristics, as is the case with real systems. We use real speech and text data sets to modify the signal. Whitening and verifying that the bits are equal is done using a block randomizer in digital modulation. A good deal of research has been done on the effects of radio channels.

We describe additive Gaussian white noise and time-varying multi-path fading of the channel impulse response. Our channel models contribute dilation, translation, uncertain scale, and impulsive noise to our synthetic signal sets<sup>(19)</sup>. The trained CNN network detects the following eight forms of digital modulation and three types of analogue modulation viz. BPSK, QPSK, 8-PSK, 16-QAM, 64-QAM, PAM4, GFSK, CPFSK, B-FM, DSB-AM and SSB-AM.

### 4.2 Effects of Channels on Modulated Signal

In a communications system, channel effects, on the other hand, are not deterministic and are not totally invertible. Real-world systems undergo a variety of impacts on the sent signal, making recovery and representation difficult. The signals are routed over a Rician multipath fading channel. Assume a [0 1.8 3.4] sample delay profile with average path gains of [0 -5 -10], [0 -6 -12] and [0 -2 -10] dB. The K-factor is 4, and the greatest Doppler shift is 4 hertz, which corresponds to a walking speed of 902 MHz.

Clock offset occurs as a result of the imperfections of transmitters and receivers' internal clock sources<sup>(20)</sup>. Clock offset deviates from the optimum values for the center frequency, which is used to down-convert the signal to baseband, and the sampling rate of the digital-to-analog converter. Each frame is frequency offset by a factor determined by the clock offset factor and the center frequency. Apply a sampling rate offset to each frame based on the clock offset factor. The parameter values in Table 1 are utilized to generate modulated signals with channel effects.

### 4.3 Training the Network

Complex signals are transformed into real-valued 4-D arrays before training the network. One page (3rd dimension) contains in-phase samples, whereas the other page (2nd dimension) has quadrature samples. Convolutional filters of  $1 \times S_{pf}$  size ensure that information in the I and Q channels is intermingled even in the convolutional layers and that phase information is more effectively utilized. Iterative training of neural networks is required. Before updating network coefficients, read data from files and convert the data. A CNN with six convolution layers and a fully connected layer is utilized. Batch normalization, rectified linear unit activation, and maximum pooling follow each convolution layer until the final. The maximum pooling layer is replaced with an average pooling layer in the final convolution layer. The output layer is activated by soft-max. Each modulation type will contain 10,000 frames, with 80% used for training, 10% for validation, and 10% for testing. Each frame has 1024 samples and is sampled at a rate of 200 kHz. Eight samples constitute a symbol in digital modulation types. Each decision is made by the network based on a single frame rather than numerous consecutive frames (as in video). Assume a central frequency of 902 MHz for digital modulation and 100 MHz for analogue modulation, respectively.

**Table 1. Data Set Parameters**

Parameter	Configuration - I	Configuration - II	Configuration - III
Centre Frequency in Hz	902000000	902000000	902000000
SNR in dB	30	10	0
Sample Rate	200000	200000	200000
Path Delays	[0 9.0000e-06 1.7000e-05]	[0 9.0000e-06 1.7000e-05]	[0 9.0000e-06 1.7000e-05]
Average Path Gains in dB	[0 -2 -10]	[0 -5 -10]	[0 -6 -12]
K Factor	4	4	4
Maximum Doppler Shift	4	4	4
Maximum Clock Offset	5	5	5
Trans Delay	50	50	50
Channel Delay	6	6	6
Maximum Frequency Offset in Hz	4510	4510	4510
Maximum Sample Rate Offset in Hz	1	1	1

#### 4.4 Experimental Setup & Testing with SDR

To evaluate the classification of Over-the-Air modulation, we employed two ADALM-PLUTO Active Learning Modules (PlutoSDR), a simple-to-use technology provided from Analog Devices Inc. (ADI) that can be used to explain the principles of software-defined radio (SDR), radio frequency (RF), or communications as advanced electrical engineering topics. Following are the steps involved in testing Over-the-Air Modulation classification using Software Defined Radios:

1. Two dedicated ADALM-PLUTO Software Defined Radio are used one for Transmission and one for Reception.
2. Both SDRs are physically separated by 3 foot and a reflecting obstacle to create real-time wireless scenario.
3. Generate signals to transmit through transmitting SDR.
4. Transmit the signal through ADALM-PLUTO SDR.
5. Capture the channel-impaired signal using an SDR receiver.
6. Predict modulation type using trained networks with the same classification function.
7. Plot Confusion Matrix.
8. Calculate Accuracy of the network.
9. Repeat for various configurations with different signal strengths.

### 5 Results and Discussions

In this section we present the performance comparison of OTA signals under various channel profiles and different hyper-parameters. We have used 11 modulation schemes out of which 8 are digital and 3 are analog with the center frequency of 902 Mhz for digital and 100 Mhz for Analog. We have used 10,000 frames and each frame will have 1024 samples and has a sample rate of 200 kHz and each sample will go through the fading channels before training out of 10,000 samples 80% samples is used for training, 10% for validation and 10% will be for testing.

Figure 3 shows the confusion matrix for test data with configuration I with reflecting obstacle between transmitter and receiver, testing sample size of 10,000 samples and Mini-Batch Size of 12 & No. of Epochs 256 & Final test accuracy is 93.8818%. It is imperative from the result that as 64QAM is subset of 16QAM accuracy decreases.

Figures 4 and 5 shows the confusion matrix for test data with configuration III in which the signals used for training are passed through a channel with path gain of [0 -5 -10] dB. Testing sample size of 1000 & 100 samples, Mini-Batch Size of 12 & 24 & No. of Epochs 256 & 128 and found Final test accuracy is 91.4545% & 97.4545% respectively.

Figures 6 and 7 shows the confusion matrix for test data with configuration III in which the signals used for training are passed through severely affected fading channels compared to configuration II i.e., channel path gain of [0 -6 -12] dB is used. Mini-Batch Size of 12 & 24 & No. of Epochs 256 & 128 and found Final test accuracy is 98.0363% & 89.2727% respectively.

CNN has been tested using TWO ADALM-PLUTO Software Defined radio hardware and Over-The-Air signals. OTA signals are generated using computer simulation similar to the one used for training the network and transmitted. Channel impairment is created by physically separating Transmitter and receiver by 3foot distance and a reflective obstacle is placed in between them.

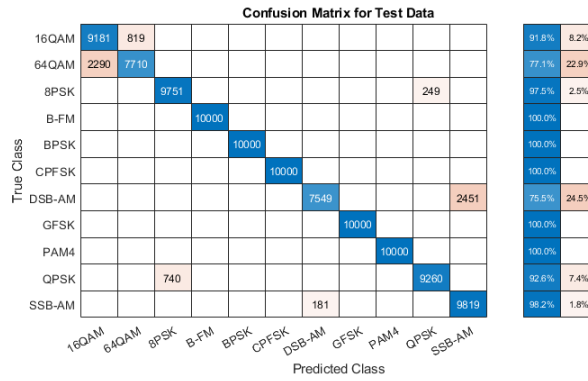


Fig 3. Confusion Matrix for Test Data with Configuration I with reflecting obstacle & Final test accuracy: 93.8818%

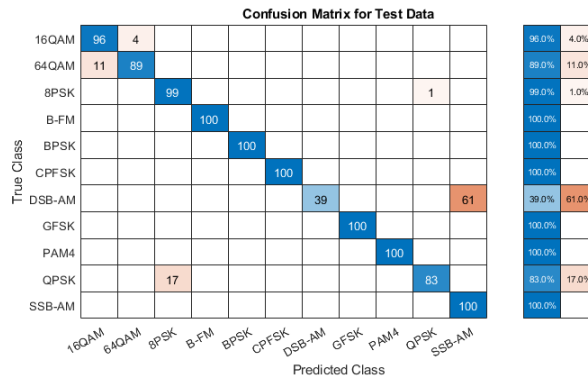


Fig 4. Confusion Matrix for Test Data with Configuration II & Final test accuracy: 91.4545%

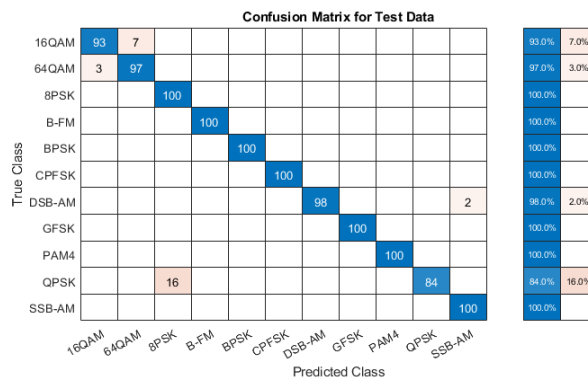


Fig 5. Confusion Matrix for Test Data with Configuration II & Final test accuracy: 97.4545%

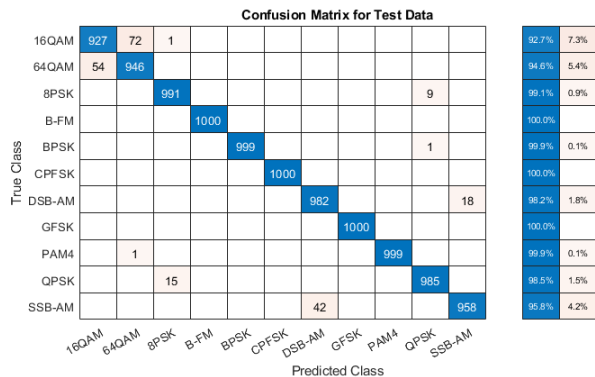


Fig 6. Confusion Matrix for Test Data with Configuration III & Final test accuracy: 98.0363%

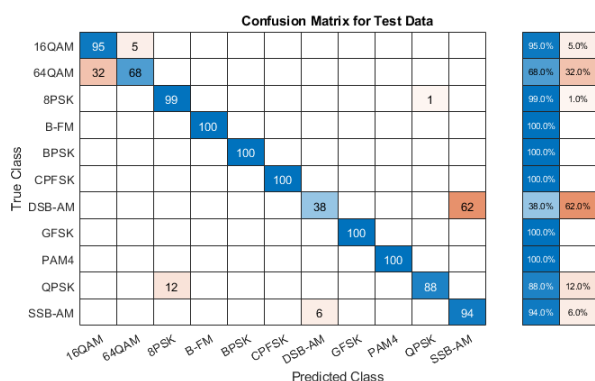


Fig 7. Confusion Matrix for Test Data with Configuration III & Final test accuracy: 89.2727%

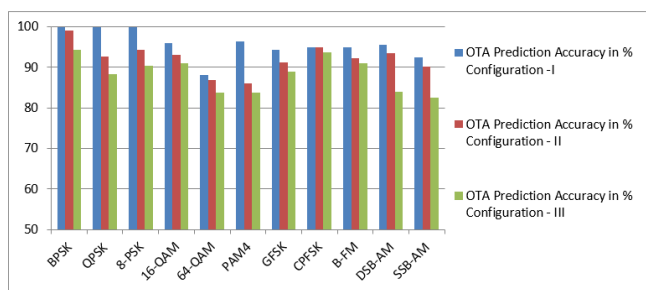
Tables 2 and 3 shows the tabulated result based on experimental setup as discussed in section 5.4. We have used two different networks to test OTA signals. Table 2 shows the accuracy of first network in which the Mini-Batch Size of 12 & No. of Epochs 256 are three different configurations with prediction accuracy of 91.4% and Table 3 shows the tabulated result of second network with Mini-Batch Size of 24 & No. of Epochs 128 with an overall prediction accuracy of 94.3%. Figures 8 and 9 are the graphical representation of the tabulated result.

Table 2. OTA Prediction Accuracy with Mini-Batch Size of 12 & No. of Epochs 256

Modulation Type	OTA Prediction Accuracy in %		
	Configuration -I	Configuration - II	Configuration - III
BPSK	100	99	94.3
QPSK	100	92.7	88.23
8-PSK	100	94.21	90.4
16-QAM	96	93	90.98
64-QAM	88	86.9	83.65
PAM4	96.3	86	83.73
GFSK	94.28	91.14	89
CPFSK	95	94.87	93.75
B-FM	94.9	92.14	91.1
DSB-AM	95.46	93.45	84
SSB-AM	92.5	90.2	82.5

**Table 3. OTA Prediction Accuracy with Mini-Batch Size of 24 & No. of Epochs 128**

Modulation Type	OTA Prediction Accuracy in %		
	Configuration - I	Configuration - II	Configuration - III
BPSK	100	100	99
QPSK	100	96.3	94.0
8-PSK	100	96.7	95.67
16-QAM	100	95.48	95.5
64-QAM	92	91.80	90
PAM4	93.3	93.17	91.67
GFSK	97.44	94.66	92.85
CPFSK	98.85	93.42	91.6
B-FM	98	96.5	94
DSB-AM	97	95.45	88.8
SSB-AM	95.45	93.88	89.27



**Fig 8. Comparative Analysis of Prediction accuracy under different channel configurations with Mini-Batch Size of 12 & No. of Epochs 256**

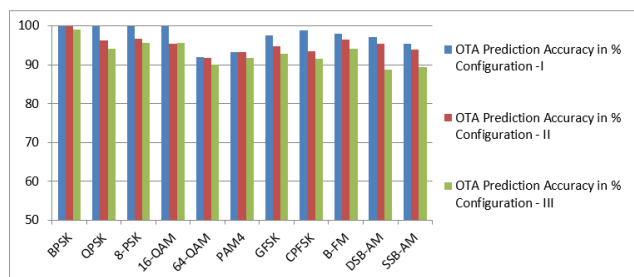


**Fig 9. Comparative Analysis of Prediction accuracy under different channel configurations with Mini-Batch Size of 24 & No. of Epochs 128**

It is clear from the data presented above that modulation recognition at low SNR will be a difficult undertaking to accomplish. It has been discovered that when the parameters provided in various configurations with first CNN<sup>(7)</sup> which has ReLu activation layer with 12 Mini-Batch Size and 256 Epochs are compared with the second CNN which also make use of ReLu activation layer but with 24 Mini-Batch Size and 128 Epochs under various channel circumstances that approximately an improvement in OTA classification accuracy of 4 percent has occurred.

## 6 Conclusion

Modulation classification, which is a primary task of CR systems, has been accomplished well utilizing deep learning algorithms. The experimental results indicate that by adjusting the hyper-parameters, the classification accuracy may be increased by almost

4% in this experimental configuration. However, the difficulty of modulation classification persists, as modern transceivers that employ adaptive modulation schemes in response to channel circumstances have a very narrow classification margin when modulation schemes are changed. As an illustration, we used QAM64, a variation of QAM16, which demonstrates resistance to correctly identifying the modulation scheme. Additionally, this study can be expanded by first obtaining real-time signals and then using them for training, resulting in more realistic outcomes.

## References

- 1) Danesh K, Vasuhi S, S. An effective spectrum sensing in cognitive radio networks using improved convolution neural network by glow worm swarm algorithm. *Transactions on Emerging Telecommunications Technologies*. 2021;32(11):e4328–e4328. Available from: <https://doi.org/10.1002/ett.4328>.
- 2) López D, Rivas E, Gualdron O. Primary user characterization for cognitive radio wireless networks using a neural system based on Deep Learning. *Artificial Intelligence Review*. 2017;52(1):169–195. doi:10.1007/s10462-017-9600-4.
- 3) Gravelle C, Zhou R. SDR Demonstration of Signal Classification in Real-Time Using Deep Learning. *2019 IEEE Globecom Workshops (GC Wkshps)*. 2019;p. 1–5. doi:10.1109/GCWkshps45667.2019.9024661.
- 4) Li W, Zhang K, Lei W, Shen R. Dynamic cooperative spectrum sensing in cognitive radio networks. *2011 International Conference on Computational Problem-Solving (ICCP)*. 2011;10:1354–1358. doi:10.1109/iccps.2011.6089785.
- 5) Jdid B, Hassan K, Dayoub I, Lim WH, Mokayef M. Machine Learning Based Automatic Modulation Recognition for Wireless Communications: A Comprehensive Survey. *IEEE Access*. 2021;9:57851–57873. doi:10.1109/ACCESS.2021.3071801.
- 6) Goyal SB, Bedi P, Kumar J, Varadarajan V. Deep learning application for sensing available spectrum for cognitive radio: An ECRNN approach. *Peer-to-Peer Networking and Applications*. 2021;14:3235–3249. doi:10.1007/s12083-021-01169-4.
- 7) Stephan T, Al-Turjman F, J S, Balusamy B. Energy and spectrum aware unequal clustering with deep learning based primary user classification in cognitive radio sensor networks. *International Journal of Machine Learning and Cybernetics*. 2021;12(11):3261–3294. doi:10.1007/s13042-020-01154-y.
- 8) O'shea TJ, Roy T, Clancy TC. Over-the-Air Deep Learning Based Radio Signal Classification. *IEEE Journal of Selected Topics in Signal Processing*. 2018;12(1):168–179. doi:10.1109/jstsp.2018.2797022.
- 9) Wang Y, Liu M, Yang J, Gui G. Data-Driven Deep Learning for Automatic Modulation Recognition in Cognitive Radios. *IEEE Transactions on Vehicular Technology*. 2019;68(4):4074–4077. doi:10.1109/tvt.2019.2900460.
- 10) Hanna S, Dick C, Cabric D. Signal Processing Based Deep Learning for Blind Symbol Decoding and Modulation Classification. *IEEE Journal on Selected Areas in Communications*. doi:10.1109/JSAC.2021.3126088.
- 11) Lu H, Bo L. WDLReconNet: Compressive Sensing Reconstruction With Deep Learning Over Wireless Fading Channels. *IEEE Access*. 2019;7:24440–24451. doi:10.1109/access.2019.2900715.
- 12) Awe OP, Babatunde DA, Lambotharan S, Assadhan B. Second order Kalman filtering channel estimation and machine learning methods for spectrum sensing in cognitive radio networks. *Wireless Networks*. 2021;27:3273–3286. doi:10.1007/s11276-021-02627-w.
- 13) Zheng S, Chen S, Qi P, Zhou H, Yang X. Spectrum sensing based on deep learning classification for cognitive radios. *China Communications*. 2020;17(2):138–148. doi:10.23919/JCC.2020.02.012.
- 14) Nasser A, Chaitou M, Mansour A, Yao KC, Charara H. A Deep Neural Network Model for Hybrid Spectrum Sensing in Cognitive Radio. *Wireless Personal Communications*. 2021;118(1):281–299. doi:10.1007/s11277-020-08013-7.
- 15) Nasser A, Chaitou M, Mansour A, Yao KC, Charara H. A Deep Neural Network Model for Hybrid Spectrum Sensing in Cognitive Radio. *Wireless Personal Communications*. 2021;118(1):281–299. doi:10.1007/s11277-020-08013-7.
- 16) Xu T, Darwazeh I. Deep Learning for Over-the-Air Non-Orthogonal Signal Classification. *2020 IEEE 91st Vehicular Technology Conference (VTC2020-Spring)*. 2020;p. 1–5. doi:10.1109/VTC2020-Spring48590.2020.9128869.
- 17) Ahmed R, Chen Y, Hassan B. Deep residual learning-based cognitive model for detection and classification of transmitted signal patterns in 5G smart city networks. *Digital Signal Processing*;120:2022–2022. doi:10.1016/j.dsp.2021.103290.
- 18) Li X, Fang J, Cheng W, Duan H, Chen Z, Li H. Intelligent Power Control for Spectrum Sharing in Cognitive Radios: A Deep Reinforcement Learning Approach. *IEEE Access*. 2018;6:25463–25473. doi:10.1109/access.2018.2831240.
- 19) Chauhan PS, Kumar S, Upadhyay VK, Mishra R, Kumar B, Soni SK. Performance analysis of ED over air-to-ground and ground-to-ground fading channels: A unified and exact solution. *AEU - International Journal of Electronics and Communications*;138:2021–2021. doi:10.1016/j.aeu.2021.153839.
- 20) O'mahony GD, McCarthy KG, Harris PJ, Murphy CC. Developing a Low-Order Statistical Feature Set Based on Received Samples for Signal Classification in Wireless Sensor Networks and Edge Devices. *IoT*;2021:449–475. doi:10.3390/iot2030023.